Targeting the osteoclastogenic cytokine IL-9 as a novel immunotherapeutic strategy in mitigating inflammatory bone loss in post-menopausal osteoporosis

Leena Sapra[1], Chaman Saini[1], Shivani Sharma[2], Dibyani Nanda[1], Aishwarya Nilakhe[3], Naibedya Chattopadhyay[2] , Avtar Singh Meena[1], Pradyumna K. Mishra[4], Sarika Gupta[3], Bhavuk Garg[5], Vikrant Manhas[5], Rupesh K. Srivastava[1,*]

[1]Translational Immunology, Osteoimmunology & Immunoporosis Lab (TIOIL), Department of Biotechnology, All India Institute of Medical Sciences (AIIMS), New Delhi 110029, India
[2]Division of Endocrinology, Central Drug Research Institute (CDRI), Lucknow 226031, India
[3]National Institute of Immunology (NII), New Delhi 110067, India
[4]Department of Molecular Biology, ICMR-National Institute for Research in Environmental Health, Bhopal, MP 462001, India
[5]Department of Orthopaedics, All India Institute of Medical Sciences (AIIMS), New Delhi 110029, India
*Corresponding author: Rupesh K. Srivastava, Translational Immunology, Osteoimmunology & Immunoporosis Lab (TIOIL), Department of Biotechnology, All India Institute of Medical Sciences (AIIMS), New Delhi 110029, India (rupesh_srivastava13@yahoo.co.in, rupeshk@aiims.edu).

Abstract

Recent discoveries have established the pivotal role of IL-9-secreting immune cells in a wide spectrum of inflammatory and autoimmune diseases. However, little is known about how IL-9 contributes to the etiology of inflammatory bone loss in PMO. We observed that IL-9 has a pathological impact on inflammatory bone loss in ovariectomized (Ovx) mice. Our in vivo temporal kinetics analysis revealed that estrogen deprivation enhanced the production of IL-9 from Th cells (majorly Th9 and Th17). Both our ex vivo and in vivo studies corroborated these findings in Ovx mice, as estrogen diminishes the potential of Th9 cells to produce IL-9. Mechanistically, Th9 cells in an IL-9-dependent manner enhance osteoclastogenesis and thus could establish themselves as a novel osteoclastogenic Th cell subset. Therapeutically neutralizing/blocking IL-9 improves bone health by inhibiting the differentiation and function of osteoclasts, Th9, and Th17 cells along with maintaining gut integrity in Ovx mice. Post-menopausal osteoporotic patients have increased IL-9-secreting Th9 cells, which may suggest a potential role for IL-9 in the development of osteoporosis. Collectively, our study identifies IL-9-secreting Th9 cells as a driver of bone loss with attendant modulation of gut-immune-bone axis, which implies IL-9-targeted immunotherapies as a potential strategy for the management and treatment of inflammatory bone loss observed in PMO.

Keywords: Th9 cells, Th17 cells, Il-9, Il-17, osteoporosis, immunoporosis, gut, osteoclast and bone health
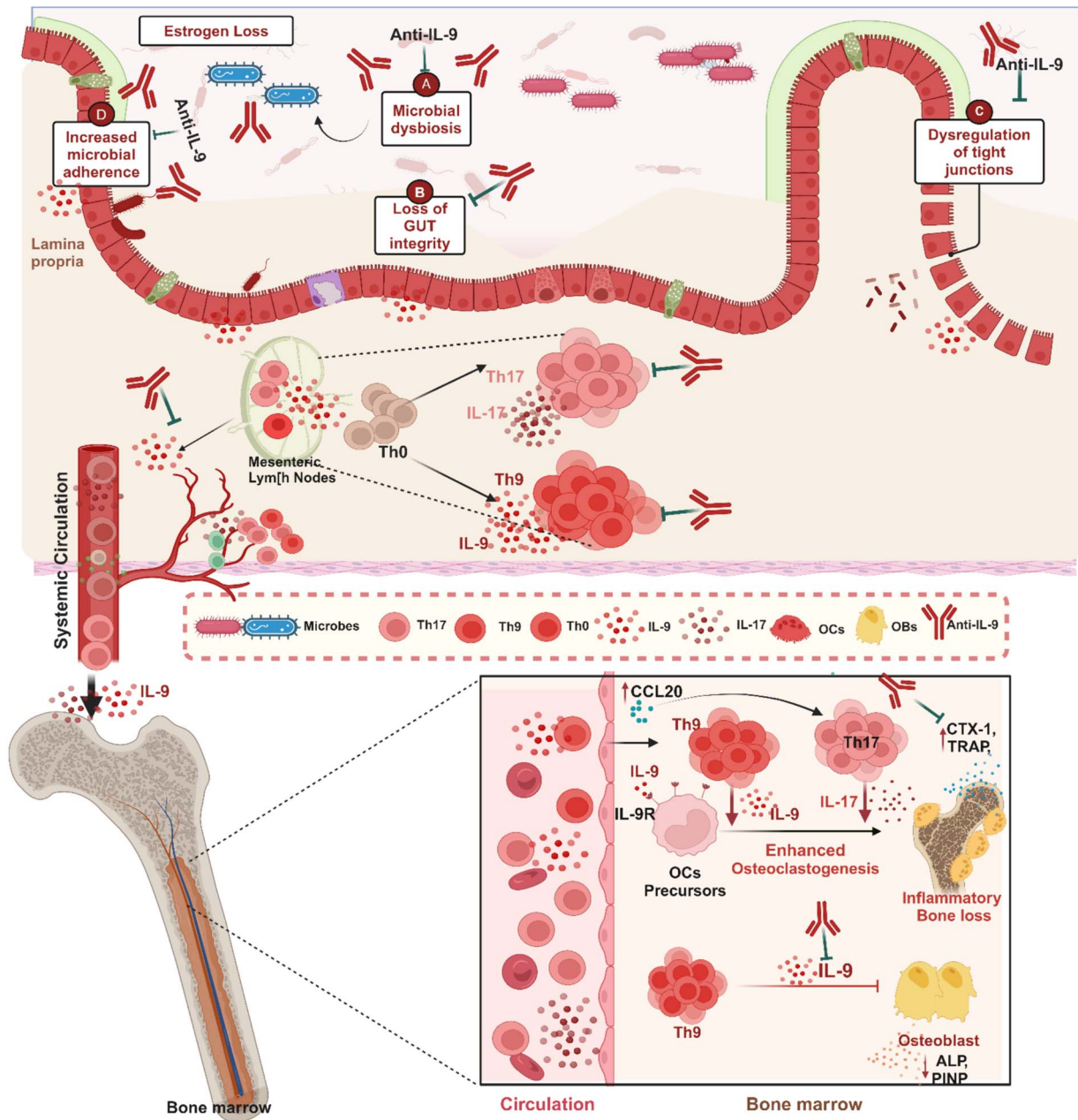
Lay Summary

Our research identifies interleukin-9 (IL-9) as a key driver of bone loss in PMO. By promoting osteoclast formation and suppressing bone formation, IL-9 significantly contributes to the disease's progression. Our findings in both animal models and human patients suggest that targeting IL-9 could provide a novel therapeutic approach to combat bone loss in postmenopausal women.

Graphical Abstract

Introduction

Osteoporosis is a systemic skeletal illness that is principally distinguished by a loss of bone mechanical strength (BMS) and bone mineral density (BMD), thereby raising the risk of fragility-related fractures in the wrist, hip, and spine.[1,2] It is the fourth most burdensome chronic disease after ischemic heart disease, dementia, and lung cancer, impacting over 500 million people globally.[3] PMO is a common skeletal disorder that increases the risk of fragility fractures and attendant morbidity. Postmenopausal bone loss is linked to chronically low-grade inflammation primarily because of the role played by estrogen on the immune system.[4] Estrogen has anti-inflammatory effects and regulate the activity of immune cells in manners that downregulates the production of pro-inflammatory cytokines such as interleukin (IL)-6, TNFα,

and IL-17.[5] These pro-inflammatory cytokines activate osteoclasts leading to greater bone breakdown over formation.

The role of T cells in the pathogenesis of bone loss is an emerging field of research with no clear consensus. Some studies reported that T cells may not be essential to the pathogenesis of estrogen deficiency-induced bone loss.[6-8] By contrast other reports demonstrated that T cells are vital in inducing bone loss under estrogen deficiency.[9-18] Moreover, bone loss caused by low estrogen and parathyroid hormone (PTH) has been linked to IL-17 producing Th17 cells,[19] as increased expression of IL-17 stimulated the expression and activity of receptor activator of nuclear factor kappa B ligand (RANKL), resulting in enhanced bone loss.[19] We and others have demonstrated that the disruption of the homeostatic balance between the osteoclastogenic Th17 cells and anti-osteoclastogenic

Tregs cells is one of the major underlying mechanisms of bone loss in PMO.[9-11] Distinct subsets of Th cells, each with their own unique cytokine profile and functional properties, define the nature of their immune responses. One such subset of T helper cells that mainly secretes the pro-inflammatory IL-9 cytokine was discovered and was later named as "Th9 cells" in 2008.[20] Th9 cell differentiation is predominantly induced by the cytokines transforming growth factor-beta 1 (TGFβ-1) and IL-4. Additionally, forkhead family transcription factor (FOXO1) and interferon regulatory factor 4 (IRF4) are essential for the growth and function of Th9 cells.[21-23]

Th9 cells enhance immunological tolerance and afford protection against parasitic infections.[24] They also have potent anti-tumor immunity, making them a potential candidate for cancer immunotherapy. Conversely, Th9 cells contribute to widespread allergic inflammation, asthma, and autoimmune diseases, highlighting their pathogenic roles in a range of immunological disorders.[25] Furthermore, the presence of Th9 cells and the related production of IL-9 in the synovial fluid and PBMCs of RA patients indicate that IL-9 may be involved in the inflammatory processes within the joints affected by RA.[26] These findings indicate that inhibiting IL-9 signaling could be a viable strategy for limiting the inflammatory deterioration of bone, not just in RA but also in PMO. Interestingly the nexus between gut microbiota (GM), immune system, and bone health (ie, Osteomicrobiology) is now well studied.[23,24] Dysbiosis of the GM and subsequent loss of intestinal barrier integrity promotes the occurrence of distinct degenerative skeletal diseases including osteoporosis.[27-29] Of note, dysbiosis of GM in ulcerative colitis and sepsis patients is further linked with enhanced levels of IL-9.[30-32] However, the regulation of "Th9-IL-9" axis along with their association with GM in PMO is largely unknown.

We thus hypothesized that estrogen deficiency-mediated dysbiosis would lead to enhanced production of IL-9, thereby paving path for alleviation of inflammatory bone loss in PMO. We addressed this hypothesis by examining the "Gut-Immune-Bone" axis in pre-clinical mice model of PMO. Both our murine and human data collectively demonstrates the pathological role of "Th9-IL-9" axis in triggering inflammatory bone loss (linked with dysbiosis of GM) under estrogen deficient conditions. Our findings could open up novel therapeutic avenues for IL-9 targeted immunotherapy in PMO.

Materials and methods
Reagents and antibodies
The following antibodies were procured from Biolegend (United States): PerCp-Cy5.5-Anti-Mouse-CD4-(RM4-5) (550954), BV786-Anti-Mouse-IL-17A-(506928), BV421-Anti-Mouse-IL-9-(514109), BV711-Anti-Mouse-IL-4-(504133), BV605-Anti-Mouse-IFNγ-(505839) etc. Foxp3/ Transcription factor staining buffer (0-5523-00) and RBC lysis buffer (00-4300-54) were purchased from eBioscience. Acid phosphatase, leukocyte (TRAP) kit (387A) was purchased from Sigma (United States). Human TGF-β1 (AF-100-21C), IL-9 (219-19), and IL-4 were procured from PeproTech (United States). Anti-CD3 and Anti-CD28 were purchased from BD (United States). α-Minimal essential media (MEM) and RPMI-1640 were purchased from Gibco (United States). Following ELISA kits were brought from R&D: Mouse IL-10 (M1000B) and Mouse IL-17 (M1700) Quantikine ELISA kits. The following ELISA kits and reagents were brought from BD

(United States): Mouse IL-6 (OptEIA-555 240), Mouse TNF-α (OptEIA-560 478), and Mouse IL-9. Anti-IL-9 was purchased from BioXcell (United States).

Post-menopausal osteoporotic mice model
All in vitro and in vivo studies were performed on female C57BL/6 mice (8 to 10 wk old). All the mice were kept in specified pathogen-free environments at the animal facility of All India Institute of Medical Sciences (AIIMS), New Delhi, India. For the investigation and kinetic study, following groups: sham (control-ovaries intact) and ovariectomized (Ovx) (n = 6/grp) were employed for 3 time periods (15, 30, and 45 d). Surgery was carried out according to the previous studies.[33] After respective time periods, mice were euthanized by CO_2 asphyxiation and blood, bones and lymphoid tissues (BM, spleen, and MLN) were harvested. For IL-9 blockade, mice were injected intra peritoneally (i.p) with 200 μg/mice anti-IL-9 antibody every other day starting on day -1 of Ovx surgery, another group received isotype-matched IgG at a dose of 200 ug/mice on day -1 of Ovx surgery for day 45. All the procedures were carried out in accordance with the guiding principles, suggestions, and after the protocol was approved by the institutional animal ethics committee of AIIMS, New Delhi, India (384/IAEC-1/2022).

Scanning electron microscopy
As previously reported[33,34] SEM was done for the cortical area of the femoral bones. Briefly, bone samples were stored in 1 % Triton-X-100 for 3 d and stored in 1 % PBS buffer. SEM images were captured at 100× magnification. MATLAB was used to further analyze the SEM pictures (MathWorks, Natick, MA, United States).

16S rRNA microbial community analysis
At day 45, fecal pellets from mice of different groups were collected and stored in −80°C for metagenome-analysis. DNA-extraction, quantity and library was prepared as per manufacturer's protocol (Illumina Kit, NEBNext #E7645S/L). Final libraries were quantified using Qubit 4.0 fluorometer (Thermofisher #Q33238) using DNA HS assay kit (Thermofisher #Q32851) following manufacturer's protocol. Relative abundance was calculated based on the taxonomic classification. Alpha rarefaction curve and alpha (parameters: - group = sample types, measures = Chao1, Shannon, Simpson, ACE, observed Operational taxonomic units (OTUs), Pielou) was plotted using Microbiota Process R packages.

Intestinal permeability assay
Intestinal permeability was evaluated by FITC-dextran assay. Mice were deprived of food and water for 4 h and were orally gavaged with 200 ul of 1XPBS (containing 80 mg/mL FITC dextran) and were further deprived of food and water for next 4 h. FITC dextran was estimated in the plasma sample via fluorescence intensity using an excitation wavelength of 488 nm and an emission wavelength of 528 nm via employing a NanoDrop spectrophotometer/fluorimeter (BioTek Synergy H1).

Micro-computed tomography
Micro CT (μ-CT) scanning and analysis were done by employing in vivo X-ray SKYSCAN 1076 scanner (Aartselaar, Belgium) tomography as previously reported by our group.[35]

Briefly, first, samples were positioned correctly in the sample holder before scanning was conducted at 50 kV, 204 mA, and a 0.5 mm aluminum filter. Then reconstruction was carried out followed by the evaluation of micro-architectural parameters. The measurements of bone volume/tissue volume (BV/TV), trabecular thickness (Tb. Th), trabecular separation (Tb. Sp), and other 3D-histomorphometric parameters were obtained. The BMD of the LV5, femur, and tibia were calculated using the volume of interest from u-CT scans made for trabecular and cortical regions.

Goldner trichome staining

Goldner trichome (GT) staining and imaging was carried out for unmineralized sections of femoral bones. Histomorphometric parameters viz. osteoid volume (OV), osteoid volume per bone volume (OV/BV), osteoid surface (OS), osteoid surface per bone surface (OS/BS), osteoid width (O.Wi) were evaluated via employing osteo software (Bioquant Image Analysis, Nashville TN).

Histological analysis

Paraffin-embedded sections (5 μm) from tissues were processed for the histological hematoxylin (H) and eosin (E) staining analysis. Sections were imaged using a microscope.

Th9 and Th17 cell differentiation

Splenic naïve T cells from C57BL/6 mice were purified by magnetic separation described previously.[34] Briefly, untouched negatively selected CD4$^+$CD25$^-$ naïve T cells (purity >95 %) were seeded in anti-CD3 (10 μg/mL) and anti-CD28 (2 μg/mL) mAbs coated 48 well plate. For Th9 cell differentiation, cells were cultured in RPMI-1640 media and polarized with IL-4 (20 ng/mL), TGF-β1 (5 ng/mL), and anti-IFN-γ (5 μg/mL) in the presence or absence of 17β-estradiol (1, 10, and 100 nM) and incubated for 3 d. For Th17 cell differentiation, naïve T cells were stimulated with TGF-β1 (2 ng/mL), IL-6 (30 ng/mL), IL-23 (20 ng/mL), anti-IL-4 (10 μg/mL), and anti-IFN-γ (10 μg/mL) and incubated for 3 d. At the end of incubation, cells were harvested, and flow-cytometry was performed for estimating the percentages of CD4$^+$IL-9$^+$Th9 cells.

Osteoclasts differentiation and co-culture with Th9 cells

Bone marrow cells (BMCs) were harvested from the femur/tibiae of 8–10-wk-old mice. Following RBC lysis, cells were cultured for overnight in a T-25 flask using endotoxin-free-MEM media (10 % FBS) supplemented with M-CSF (35 ng/mL). Next day, non-adherent cells (BMCs) were collected and cultured with IL-9/co-cultured with Th9 cells or Th0 cells in a 96 well plate at 1:1 cell ratio for 4 d in the presence of M-CSF (30 ng/mL) and RANKL (60 ng/mL). TRAP staining was carried out according to the manufacturer's recommendations and multinucleated TRAP-positive cells counted, imaged (ECLIPSE, TS100, Nikon), and area measured using Image-J software (NIH, United States).

Alkaline phosphatase staining

BMCs (50 000) were seeded in the 96 well plate in the presence of osteogenic induction media (OIM) comprising α-MEM supplemented with β-glycerophosphate (10 mM) and ascorbic acid (50 μg/mL) for 24 h. On day 3, 80% of the media was replenished with the fresh OIM and cells were treated with IL-9 at different concentrations. On the 7th day, alkaline phosphatase (ALP) staining was carried out with nitro blue tetrazolium (NBT)/ 5-bromo-4-chloro-3-indolyl-phosphate (BCIP) substrate as per manufacturer's protocol, images were captured (ECLIPSE, TS100, Nikon) and area of ALP-positive cells was measured using Image-J software (NIH, United States).

Flow cytometry

For intracellular cytokine analysis, cells were harvested and stimulated for 5 h with PMA (50 ng/mL, Sigma Aldrich) and Ionomycin (1 ug/mL, Sigma Aldrich) along with protein transport inhibitor (Monensin) (Biolegend, United States), and stained for specific cell surface and intracellular markers. Flow cytometry analysis was performed according to the previously defined methodologies.[33] Cells were surface stained for Th9 and Th17 cells (anti-CD4-PerCP-Cy5.5) and incubated for 30 min in the dark on ice. Cells were washed, fixed, and permeabilized with 1X fixation permeabilization buffer following surface staining. Finally, intracellular staining was performed, with BV421-conjugated-anti-IL-9 and BV786-conjugated-anti-IL-17 antibody. After washing, cells were acquired on BD FACSymphony (United States) and analyzed using Flow Jo 10 (Tree Star, Woodburn, OR, United States) software. Furthermore, to refine the differences between the samples, we carried out high dimensional t-SNE analysis (t-distributed Stochastic Neighbor Embedding) to map multiple dimensions. To improve the tSNE algorithm output we first excluded the doublets, dead cells and debris and then gated on CD3$^+$/CD4$^+$ T cells and then further selected parameters (viz. IL-9) for tSNE calculation. To further run the algorithm 1000 iterations were taken and the gated populations were displayed on the Layout editor.

Study subjects

After being screened using Dual Energy X-Ray Absorptiometry (DEXA), clinicians involved in the study have chosen the study participants. Women who had a history of smoking, drinking, endocrinopathy, diabetes, or hypertension, were pregnant or nursing, taking oral contraceptives, glucocorticoids, hormone replacement therapy, or were taking any medications that affected bone mass or the immune system were excluded from the study. Inclusion criteria for the study included normotensive, physically active, non-smoker, and non-drinker women. Prior to enrolment, postmenopausal women had experienced natural menopause for at least a year. Each participant provided their written, informed consent before having their clinical history documented. All the measures were carried out following the proper clearance of the protocols filed to the institute Ethics Committee for Post Graduate Research (IECPG-482), AIIMS, New Delhi, India. In accordance with WHO guidelines, the chosen postmenopausal women were categorized as normal (T score > -1.0 at both sites), osteopenic (T score between -1.0 and -2.5 at any site), and osteoporotic (T score < -2.5 at any site). Total 20 patients were recruited: 10 in each group in both healthy control (HC) and postmenopausal osteoporotic (PMO) subjects. Each participant gave consent to the drawing of 10 mL of blood into heparinized tubes. PBMCs, isolated from the blood, were used immediately for flow cytometry and transcriptional analysis.

Quantitative PCR

RNA was extracted from the bone marrow cells using the RNeasy Mini Kit (Qiagen, United States) according to the manufacturer's instructions. For complimentary DNA conversion, 1 μg of total RNA was used. Furthermore, gene expression was measured using quantitative real-time (Applied Biosystems, Quantstudio-5, United States). Triplicate samples of cDNA from each group were amplified with customized primers viz. IL-9, IL-9R, IL-17A, ROR-γt, IRF4, FOXO-1, Cathepsin K, RANKL, OPG, and CCL20 normalized with arithmetic mean of GAPDH housekeeping gene. 25 ng of c-DNA was used per reaction in each well containing the 2X SYBR green PCR master mix (Promega, United States) along with appropriate primers. Threshold cycles values were normalized and expressed as relative gene expression.

Human osteoclast differentiation from PBMCs

Osteoclasts differentiation was carried out in human PBMCs according to the protocol previously reported by our group.[35] Briefly, obtained PBMCs were seeded at a density of 1X 10^6 cells per well in a 96-well plate, incubated for 2 h in a humidified 5 % CO_2 incubator and later washed twice with α-MEM (without FBS). As soon as cells adhered, they were incubated with complete α-MEM media supplemented with M-CSF (30 ng/mL) and RANKL (100 ng/mL) in the presence or absence of IL-9 cytokine at various concentrations. The plate was then incubated for the following 14 d in a CO_2 incubator with half media replenishment every third day (ie, 72 h). Following incubation, multinucleated osteoclast development was assessed using TRAP staining.

Caco-2 cell culture and barriers function

Caco-2$_{bbe2}$ cells were obtained from the American Type Culture Collection (ATCC, Manassas, VA, United States). Experiments were performed using Caco-2 cells grown in Transwell inserts (12 mm; Corning, NY, United States) for over 20 d. Caco-2 cell monolayers in Transwell inserts were treated with varying concentrations of IL-9 (0, 1, 10, and 100 ng/mL) for 96 h. Macromolecular permeability was assessed by measuring the unidirectional flux of FITC-inulin (Sigma-Aldrich, St. Louis, MO, United States). In brief, Caco-2 cell monolayers grown on Transwell inserts were challenged with varying amount of IL-9, and 20 μL of FITC-inulin (20 mg/mL) was added to the apical side. The translocation of FITC-inulin to the basal side was measured by absorbance at 485/528 nm using a Biotek Synergy H1 Plate Reader (Agilent Technologies, Santa Clara, CA, United States) after the respective treatments.

Fluorescence microscopy

Caco-2 cell monolayers was fixed in acetone and methanol solution (1:1), followed by permeabilization with 0.2% Triton X-100, blocked with BSA, and stained for tight junctions (Occludin and ZO-1) and adherens junctions (E-cadherin and β-catenin), images were captured with a Prime BSI Scientific CMOS camera (Teledyne Photometric, Tuscon, AZ, United States), analyzed with NIS Elements software (Nikon, Melville, NY, United States), and processed using ImageJ (NIH).

Statistical analysis

GraphPad Prism version 9.0 was used for statistical analysis (San Diego, CA, United States). Data were represented as mean $\pm$ SEM and $p < 0.05$ value was regarded as statistically significant. Unpaired parametric Student's t test was used to compare the 2 groups. For in vitro experiments (TRAP and Th9 cell differentiation assay), we used 3 biological replicates and 3 technical replicates. For the statistical analysis of human patient sample data, Mann–Whitney test was carried out.

Results

IL-9 levels are significantly high under estrogen deficient post-menopausal osteoporotic conditions

The study design is illustrated in (Figure S1A). Bilateral Ovx in mice resulted in nearly 3-fold decline in circulating E2 levels compared with the ovary-intact (sham surgery) control mice (Figure S1B). SEM, histological and μCT analysis of femoral and trabecular bones revealed enhanced lacunae along with a significant decrease in BMD, BV/TV, and Tb. Th in the Ovx mice compared with the sham group suggesting significantly reduced bone mass and volume (Figure S1C-I). These data suggest successful induction of our osteoporotic mice model in Ovx mice. Serum levels of osteoclastogenic cytokines such as IL-6, IL-17, and TNF-α were markedly enhanced while the levels of anti-osteoclastogenic cytokines including IL-4, IL-10, and IFN-γ were significantly decreased in the Ovx group compared with sham (Figure S2A-B), which are in line with our earlier reports.[33,34] Interestingly, serum IL-9 level was observed to be robustly increased in the Ovx mice compared with the sham and was negatively corelated with BMD (Figure 1A-B). Strikingly, the mRNA levels of both IL-9 and IL-9R were further found to be significantly enhanced in the Ovx group compared with sham (Figure 1C-D). Moreover, Foxo-1, the transcription factor that supports the differentiation of naïve CD4$^+$ T cells to IL-9 producing Th cells was further increased in the Ovx group (Figure 1E). These data clearly suggest the presence of a positive feedback loop in the bone marrow cells where increased levels of IL-9 were accompanied by a concomitant increase in its receptor and transcription factor. Altogether, our data suggest that estrogen deficiency enhances IL-9 levels in Ovx mice and thus could play a pivotal role in the observed inflammatory bone loss in PMO.

Th9 and Th17 subsets are the major source of IL-9 cytokine

IL-9 is a pleiotropic cytokine and is produced by various immune cells including ILC2, Th2, Tregs, and Th17 along with their specific cytokines. Thus, moving ahead we next sought to pinpoint the specific cellular source of IL-9 via flow cytometry in Ovx mice and found that both Th9 and Th17 are the significant source of IL-9 but not ILC2, Th2, and Tregs (Figure 1F-K) (Figure S2C-F). Interestingly, it was further observed that among the Th9 and Th17 cell population in Ovx mice it's only the IL-9$^+$IL-17$^-$Th9 cells and IL-9$^+$IL-17$^+$Th9/Th17 cells which were significantly enhanced without any marked change in the percentage of IL-9$^-$IL-17$^+$Th17 cells (Figure 1I-K). We thus next carried out temporal kinetic analysis to reveal the role of IL-9 producing Th cells (either Th9 or Th17) in the development and progression of osteoporosis (Figure 1L). We assessed
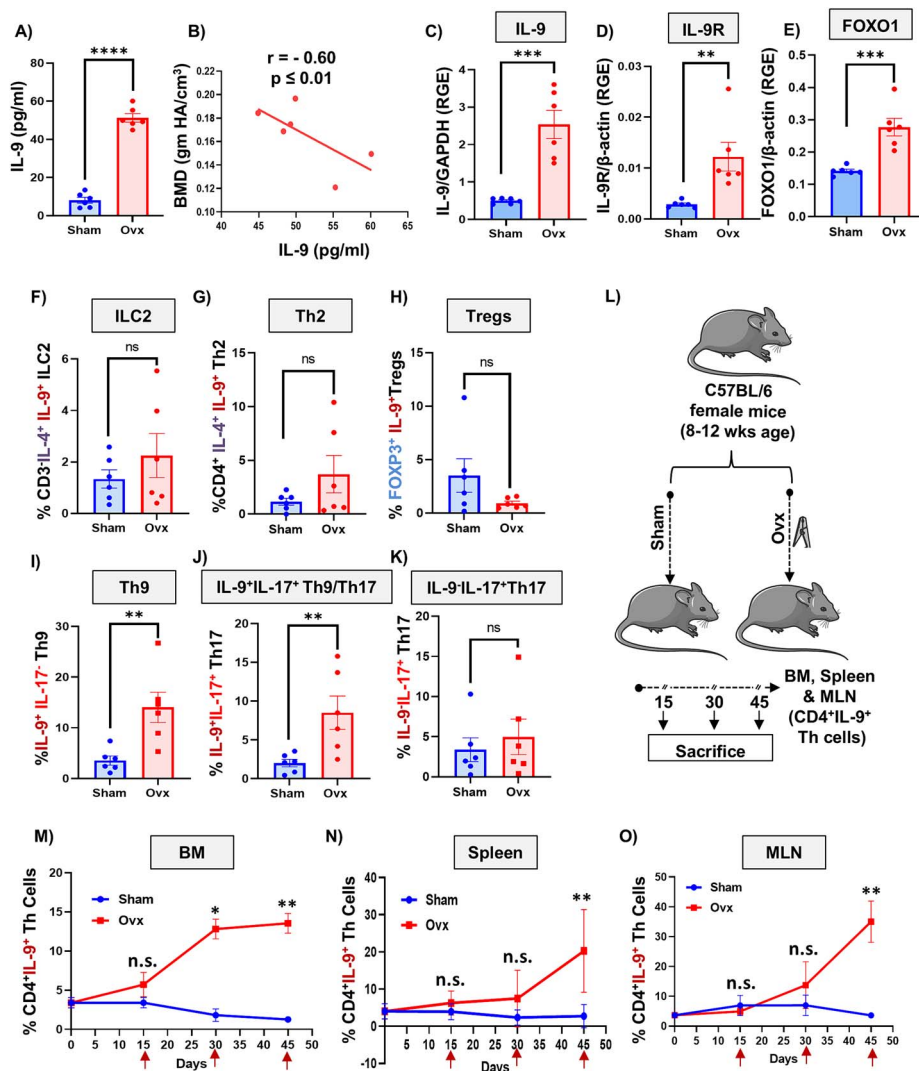
Figure 1. IL-9 cytokine levels negatively correlate with BMD: (A) Bar graphs representing IL-9 levels in the sera of sham and Ovx mice. (B) Correlation between IL-9 cytokine and BMD. (C) Relative gene expression of IL-9 gene. (D) Relative gene expression of IL-9R. (E) Relative gene expression of FOXO-1. For correlation, Pearson correlation coefficient was determined. To know the exact source of IL-9 cytokine in the Ovx condition, mice were sacrificed, and cells such as ILC2, Th2, Th17, and Tregs were analyzed for IL-9 expression in the BM. For ILC2, cells were stained with the antibody cocktail comprised of anti-CD3-PE CY7, anti-IL-4-BV711, and anti-IL-9-BV421. For Th2, cells were stained with anti-CD4-PerCpCy5.5, anti-IL-4-BV711, and anti-IL-9-BV421. For Tregs, cells were stained with anti-CD4-PerCpCy5.5, anti-Foxp3-APC, and anti-IL-9-BV421. For Th17, cells were stained with anti-CD4-PerCpCy5.5, anti-IL-17-BV786, and anti-IL-9-BV421. (F) Bar graph representing the percentage of CD3⁻IL-4⁺IL-9⁺ ILC2. (G) Bar graph representing the percentage of CD4⁺IL-4⁺IL-9⁺ Th2. (H) Bar graph representing the percentage of CD4⁺Foxp3⁺IL-9⁺ Tregs. (I) Bar graph representing percentage of CD4⁺IL-9⁺IL-17⁻ Th9 cells. (J) Bar graph representing percentage of CD4⁺IL-9⁺IL-17⁺ Th17 cells. (K) Bar graph representing percentage of CD4⁺IL-9⁻IL-17⁺ Th17 cells. (L) Cells from BM, spleen, and MLNs of sham and ovx groups were harvested and analyzed by flow cytometry for percentage of CD4⁺IL-9⁺ Th cells. (M-O) Line graph representing percentage of CD4⁺IL-9⁺ Th cells at different time periods (days 15, 30, and 45). Data are expressed as mean ± SEM. Data were analyzed by unpaired Student t test and analyzed by one-way ANOVA. *$p \leq 0.05$, **$p \leq 0.01$, ***$p \leq 0.001$, ****$p \leq 0.0001$) compared with the indicated group. Abbreviations: MLN, mesenteric lymph node; Ovx, ovariectomized.

the frequencies of IL-9⁺Th cells in the BM and secondary lymphoid organs (spleen and mesenteric lymph nodes-MLNs). We observed an increasing trend of IL-9⁺Th cells (both percentage and mean fluorescence intensity-MFI) in the BM of Ovx mice at day 15 post-Ovx, which was significantly enhanced at days 30 and 45 (Figure 1M) (Figure S3A-G). Similar results were also observed in both spleen and MLNs at day 45 post-Ovx (Figure 1N-O) (Figures S4A-G and S5A-H). The inhibitory role of estrogen on the differentiation of Th17 cells has been well established.[36] However, no study interrogated the potent role of estrogen on the differentiation of IL-9 producing Th9 cells. Strikingly, we observed that under ex vivo conditions, E2 dose-dependently inhibited

the differentiation of naïve T cells into CD4⁺IL-9⁺Th9 cells under Th9 polarization conditions (Figure 2A-C). In addition, ELISA data further demonstrated that presence of estrogen significantly reduced the capacity of Th9 cells to secrete IL-9 in the culture supernatant under ex vivo conditions (Figure 2D). These results further corroborate our above in vivo data that estrogen deficiency enhances IL-9 secreting Th9 cells in Ovx mice and thus could modulate bone health.

Th9 cells enhance osteoclastogenesis in an IL-9 dependent manner

We next investigated the role of Th9 cells on osteoclastogenesis by co-culturing BM cells with Th9 cells. Interestingly, we
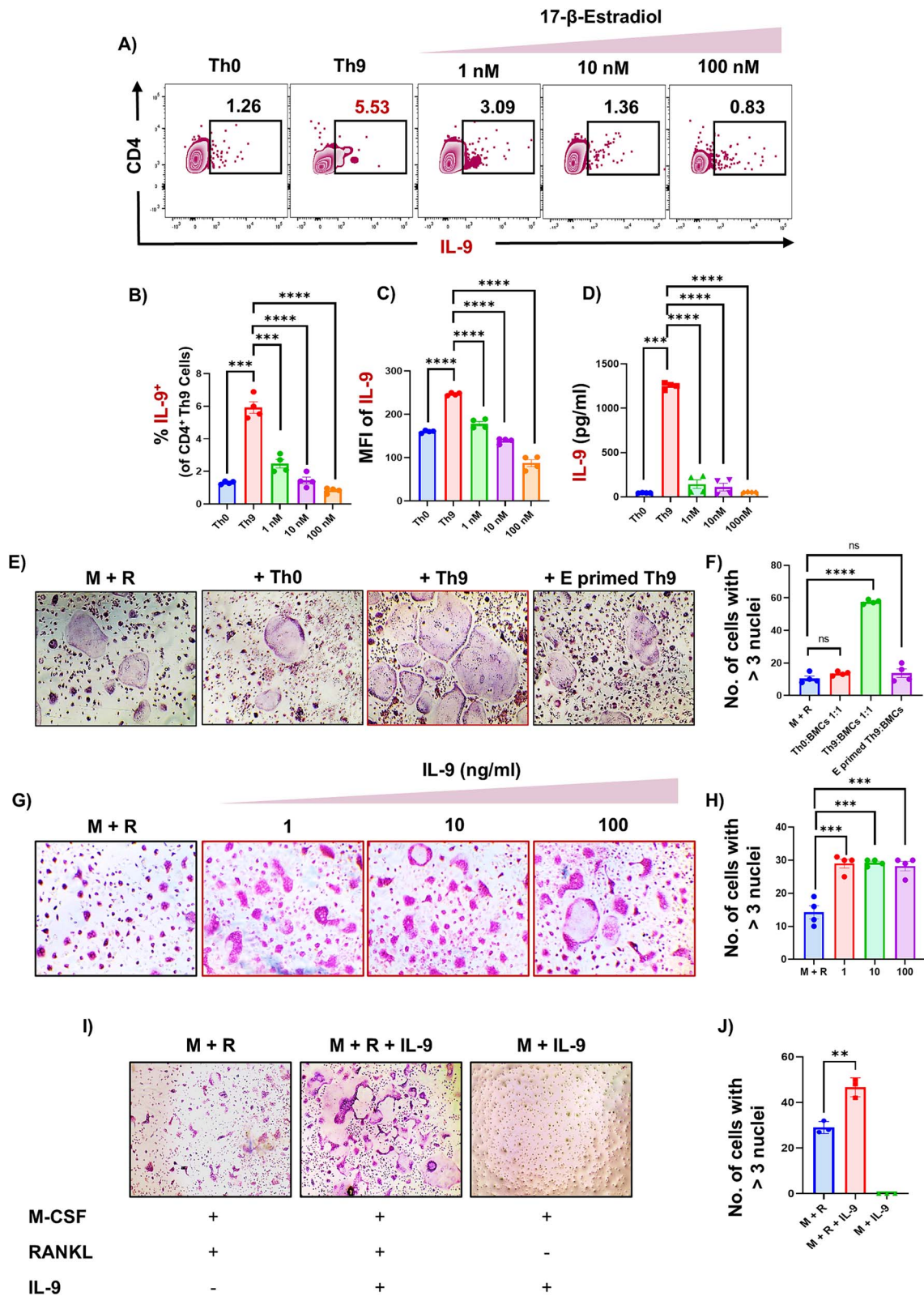
Figure 2. Th9 cells enhance osteoclastogenesis in an IL-9 dependent manner: Spleen was harvested and processed for negative selection of CD4$^+$CD25$^-$ naïve T cells. After estimation of CD4$^+$ T cells purity (>95 %), naïve T cells were cultured in Th9 differentiation conditions for 72 h. (A) Zebra plot showing the differentiation of Th9 cells in the presence of 17-β Estradiol. (B) Bar graphs representing the percentage of CD4$^+$IL-9$^+$ Th9 cells. (C) MFI of IL-9. (D) Bar graph representing the level of IL-9 in the culture supernatant of Th9 cells in the absence or presence of estrogen. (E) BMCs and Th0/Th9 were co-cultured in cell culture plate in the presence of M-CSF (30 ng/mL) and RANKL (60 ng/mL) for 4 d. Th9 cells were differentiated from naïve T cells for 72 h prior to co-cultures. Photomicrographs represent TRAP positive cells. (F) Number of TRAP positive cells with more than 3 nuclei. (G) Osteoclast differentiation was induced in BMCs with M-CSF (30 ng/mL) and RANKL (60 ng/mL) with or without IL-9 at different concentrations for 4 d. Giant multinucleated cells were stained with TRAP and cells with ≥ 3 nuclei were considered as mature osteoclasts. Photomicrographs at 20× magnification were taken. (H) Number of TRAP positive cells with more than 3 nuclei. (I) Photomicrographs represent TRAP positive multinucleated cells in absence and presence of RANKL. (J) Graph representing number of TRAP positive cells with more than 3 nuclei. Data are expressed as mean ± SEM. Data were analyzed by unpaired Student *t* test and analyzed by one-way ANOVA. *$p \le 0.05$, **$p \le 0.01$, ***$p \le 0.001$, ****$p \le 0.0001$) compared with the indicated group. Abbreviation: BMC, bone marrow cells.

observed that the number of TRAP positive multinucleated cells (with >3 nuclei) were significantly enhanced in BMCs co-cultured with Th9 cells in comparison to the control groups (Figure 2E-F). Remarkably, we further observed that Th9 cells already primed/treated with estrogen significantly inhibited the osteoclastogenic potential of Th9 cells (Figure 2E-F). We thus next sought to determine the mechanism of IL-9+Th9 cell mediated enhanced osteoclastogenesis. To ascertain this, we next examined the role of IL-9 on osteoclastogenesis under ex vivo conditions. To determine the role of IL-9 on osteoclastogenesis, we first evaluated the expression of IL-9R on monocytes (osteoclasts precursors). Both our real time and flow cytometric data demonstrated the presence of IL-9Rs on monocytes (Figure S6A-B). Interestingly, we observed that IL-9 was able to significantly enhance osteoclastogenesis, evidenced by substantial enhancement in the number of TRAP positive cells (>3 nuclei) (Figure 2G-H). Mechanistically, we observed that IL-9 induces osteoclastogenesis in a RANKL dependent manner (Figure 2I-J). These results identify IL-9 producing Th9 cells as a novel and distinct subset of osteoclastogenic Th cells, paving way for innovative immune-therapeutic targeting of IL-9 to ameliorate inflammatory bone loss in various bone pathologies including osteoporosis.

Immuno-therapeutically blocking IL-9 abrogates inflammatory bone loss under post-menopausal osteoporotic conditions

Moving ahead we immuno-therapeutically blocked IL-9 to mitigate inflammatory bone loss observed in preclinical post-menopausal osteoporotic mice model (Figure 3A). Fascinatingly, we observed that anti-IL-9 antibody effectively protected against Ovx-induced bone loss whereas isotype control failed to prevent bone loss in Ovx mice. We found that blockade of IL-9 significantly improved the microarchitecture of trabecular regions of femoral and LV-5 bones and cortical region of femoral bone (Figure 3A-B) (Figure S7A-D). Notably, blockade of IL-9 significantly enhanced the histomorphometric indices of trabecular and cortical regions viz. BMD, BV/TV, Tb.Th, Tb.No., Tt.Ar, and Tt.Pm along with significantly reducing the Tb.Sp. in Ovx mice (Figure 3C) (Figure S7A-D). Osteoid is an unmineralized bone matrix and enhancement in the OV, OV/BV, OS, OS/BS, and O.Width demonstrate impairment in the mineralization process, thereby leading to the build-up of unmineralized bone matrix (indicating reduced osteoblastogenesis). Remarkably, we observed that all these parameters were significantly altered with anti-IL-9 blockade in comparison to the Ovx group (Figure 3D-E). Anti-osteoblastogenic potential of IL-9 was further supported by the reduction in the differentiation of osteoblasts as evidenced by significant reduction in both the expression and activity of ALP in the presence of IL-9 in a dose dependent manner (Figure S7E-G). In addition, Ovx mice receiving anti-IL-9 antibody displayed significantly decreased osteoclastogenesis ex vivo (Figure 4A-B), along with reduced mRNA levels for cathepsin K, the proteinase synthesized by mature osteoclasts for degrading collagen (Figure 4C). Moreover, the osteoclastogenic/osteoblastogenic rheostat represented by *RANKL:OPG* ratio was significantly reduced upon anti-IL-9 antibody blockade (Figure 4D-F). We next evaluated the serum bone turnover markers and found that CTX-1 (bone resorption) was significantly reduced, whereas PINP (bone formation) was observed to be significantly enhanced upon IL-9 blockade in Ovx mice (Figure 4G-H). Interestingly, we observed that neutralization of IL-9 under in vivo conditions significantly reduced the percentage of both IL-9+IL-17-Th9 cells and IL-9-IL-17+Th17 cells in the BM of Ovx mice (Figure 4I-L), bringing their population below the sham levels (Figure 4I-L). Flow cytometric data further revealed similar trend in both the spleen and peripheral blood of Ovx mice post-IL-9 blockade (Figure S8A-F). Interestingly, the expression of IL-17A and Rorγt (IL-17 transcription factor), along with Foxo-1 and IRF4 (IL-9 transcription factors) were significantly decreased upon IL-9 blockade in the BM of Ovx mice (Figure 4M-P). These data clearly suggest that blocking IL-9 attenuates the differentiation/expansion of osteoclastogenic Th9 and Th17 cells in Ovx mice. In animal models of autoimmune disorders, it has been demonstrated that IL-9 not only increases Th17 cell differentiation but also facilitates Th17 cell homing by elevating CCL20 expression. Our real-time results further showed that blocking IL-9 markedly reduced *Ccl20* expression in the BM, thereby further reducing homing of osteoclastogenic Th17 cells toward BM (Figure 4Q). Altogether, our findings indicate that under post-menopausal osteoporotic conditions, IL-9 induces the differentiation/expansion and homing of osteoclastogenic Th17 cells which could further ameliorate inflammatory bone loss under estrogen deficient conditions.

Anti-IL-9 immunotherapy enhances gut-integrity and prevents dysbiosis

Dysbiosis-induced "Leaky Gut and mucosal injury" is one of the major contributing factors in PMO.[28,37] We thus next evaluated the effect of IL-9 on gut integrity under both in vitro and in vivo conditions. Interestingly, our fluorescence microscopy data demonstrated that IL-9 treatment considerably altered the expression of tight (Occludin and ZO-1) and adherens (E-cadherin and β-catenin) junctional proteins in the intestinal epithelial (Caco2) cells in a dose dependent manner (Figure 5A-B). Tight and adherens junctions regulate intestinal permeability; thus we examined the effect of IL-9 on the translocation of macromolecules in intestinal epithelial cells. Damaging effect of IL-9 on intestinal integrity was further supported by the enhanced translocation of FITC labeled inulin from the apical side toward the basal side of intestinal epithelial cells, revealing the crucial mechanism via which IL-9 may impact bone health via the "Gut-Bone" axis (Figure 6A). Moving ahead, we thus next evaluated the effect of IL-9 blockade on gut-integrity/permeability in vivo. Interestingly, our histological analysis demonstrated significantly reduced pathological damage to the colonic mucosa in the anti-IL-9 treatment group in comparison to the isotype treatment group (Figure 6B). Furthermore, the colon length (indicative of inflamed gut) was also observed to be maintained in the anti-IL-9 antibody treated group (Figure 6C-D). Of note, we observed that IL-9 blockade maintains intestinal gut-permeability in the Ovx group, as indicated by FITC-Dextran in vivo assay (Figure 6E). Furthermore, the transcriptional levels of both *claudin* and *occludin* (tight junctional proteins) were significantly higher in Ovx mice treated with IL-9 antibody (Figure 6F-G). These results indicate the pathological role of IL-9 in inducing gut-barrier disruption under estrogen deficient conditions thereby further inducing inflammatory bone loss.
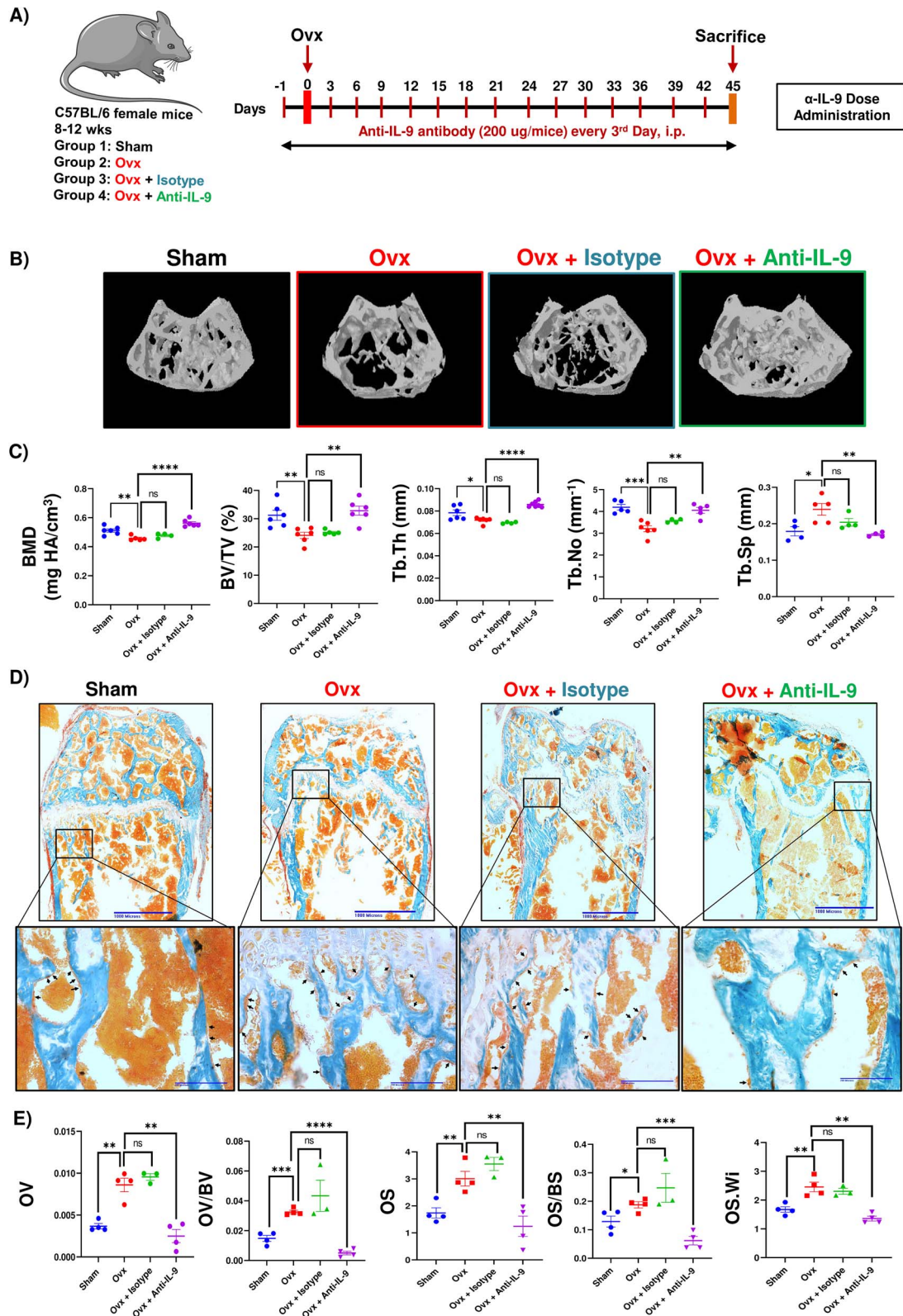
Figure 3. Anti-IL-9 immuno-therapy abrogates inflammatory bone loss under post-menopausal osteoporotic conditions: (A) Experimental plan followed for the in vivo experiment, following groups were taken including Sham, Ovx, Ovx + Isotype and Ovx + anti-IL-9 and after 45 d mice were sacrificed. (B) Micro CT data representing 3D images depicting bone microarchitecture of femur trabecular bone. (C) Plots representing the histomorphometric parameters (BMD, BV/TV, Tb.Th, Tb. No., and Tb.Sp) of femur trabecular bone. (D) Photomicrographs representing GT staining of femoral bone in different groups. (E) Static histomorphometric parameters viz. OV, OV/BV, OS, OS/BS, O.Width were quantified using osteo software (Bioquant Image Analysis, Nashville, TN). Data are expressed as mean ± SEM. Data were analyzed by unpaired Student t test and analyzed by one-way ANOVA. *$p \leq 0.05$, **$p \leq 0.01$, ***$p \leq 0.001$, ****$p \leq 0.0001$) compared with the indicated group. Abbreviations: GT, Goldner trichome; OS, osteoid surface; OS/BS, osteoid surface per bone surface; OV, osteoid volume; OV/BV, osteoid volume per bone volume; O.Width, osteoid width.
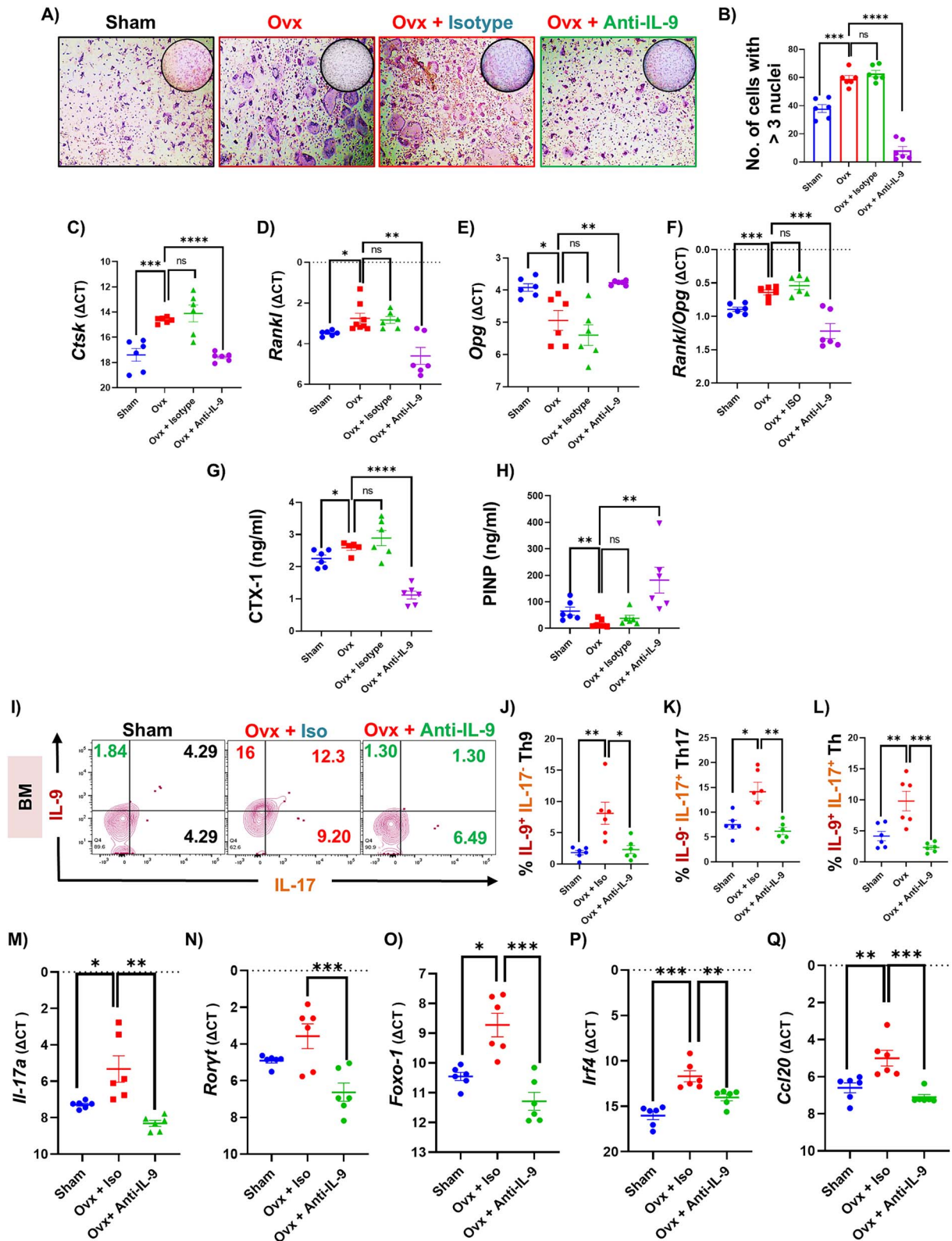
Figure 4. IL-9 blockade abrogates bone loss via modulating Th9 and Th17 cells: (A) Upon sacrifice, BMCs were harvested from all the groups and cultured in the media supplemented with M-CSF (30 ng/mL) and RANKL (60 ng/mL) and after 4 d of incubation TRAP staining was performed. (B) Number of TRAP positive cells with >3nuclei. (C-E) Bar graph representing relative expression of cathepsin K, RANKL, OPG genes in representative groups. (F) Bar graph representing RANKL/OPG ratio. (G-H) ELISA data representing the level of bone biochemical biomarkers viz. CTX-1 and PINP in the sera of respective groups. (l) Contour plots representing CD4$^+$IL-9$^+$IL-17$^+$ Th cells, CD4$^+$IL-9$^+$IL-17$^-$ Th9 cells, CD4$^+$IL-9$^-$IL-17$^+$ Th17 cells in BM. (J-L) Individual plot representing CD4$^+$IL-9$^+$IL-17$^-$ Th9 cells, CD4$^+$IL-9$^-$IL-17$^+$ Th17 cells, and CD4$^+$IL-9$^+$IL-17$^+$ Th17 cells in BM. (M-Q) Individual plots representing IL-17a, Rorγt, Foxo-1 gene expression, IRF4, and Ccl 20 gene expression in BM of representative groups. Data are expressed as mean ± SEM. Data were analyzed by unpaired Student *t* test and analyzed by one-way ANOVA. *$p \leq 0.05$, **$p \leq 0.01$, ***$p \leq 0.001$, ****$p \leq 0.0001$) compared with the indicated group. Abbreviation: IRF4, interferon regulatory factor 4.
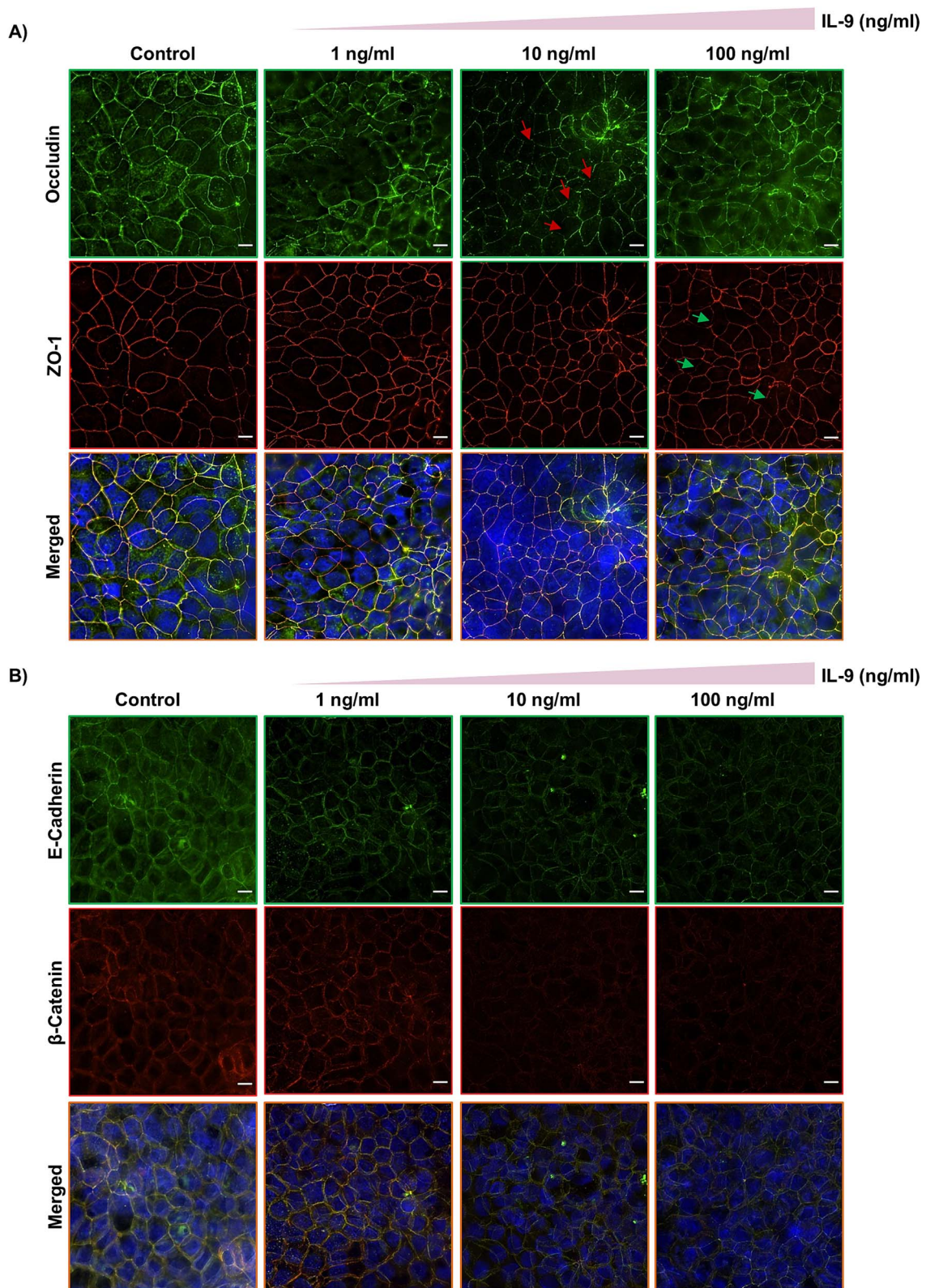
Figure 5. IL-9 induces leakiness in intestinal epithelial cells via modulating tight and adherens junction proteins: Fluorescence microscopy was carried to evaluate the expression of tight and adherens junctional proteins under in vitro conditions (A) Photomicrographs at 60× magnification were taken for tight junctional proteins (Occludin and ZO-1). (B) Photographs at 60× magnification were taken for adherens junctional proteins (E-cadherin and β-catenin). Red arrow represents occludin expression and green represents ZO-1 protein.

Leaky gut (compromised gut-integrity) is a manifestation of dysbiotic gut microbial (GM) composition under various inflammatory conditions including osteoporosis.

Thus, we next looked into the effect of IL-9 blockade on GM composition. Remarkably, we observed that IL-9 blockade maintained alpha diversity (community richness and
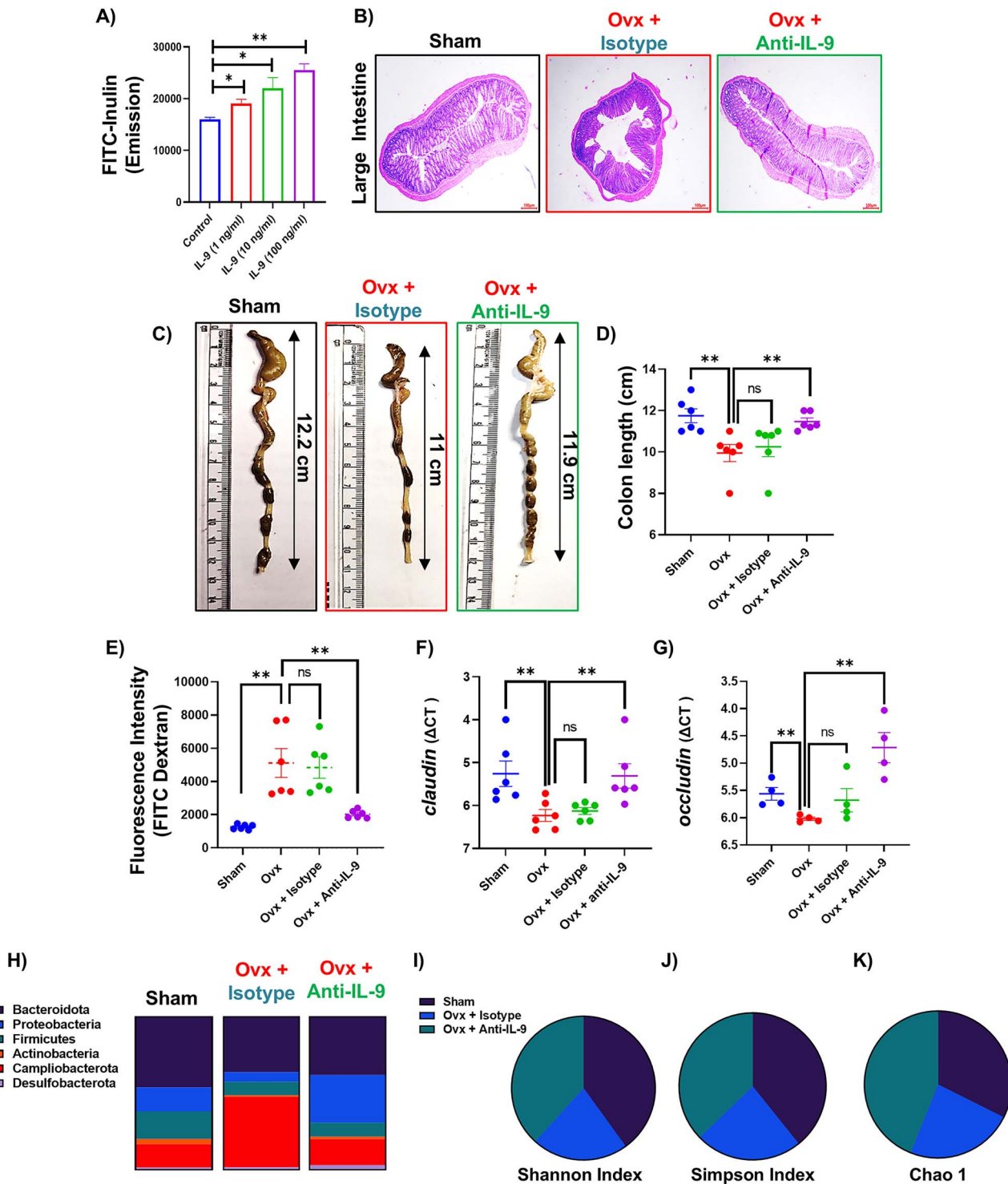
Figure 6. Blockade of IL-9 enhances GUT integrity: (A) IL-9 treatment of Caco2 cell line monolayers over a 96 h experimental period induces translocation of FITC-inulin from the apical to basal side. (B) H&E staining of large intestine tissues. (C-D) Colon length. (E) Measurement of gut integrity in sham and Ovx operated mice. FITC dextran was administered orally to each experimental mice. Fluorescence intensity was measured at excitation: 488 nm and emission 528 nm as an indicative of gut integrity. (F-G) Relative gene expression of tight junctional proteins *claudin* and *occludin* in the large intestine. (H) Stacked bar plots showing the abundance of phylum in the groups. Phyla are coded in different colors with each showing the relative abundance of that specific phylum. (I) Pie chart showing the various alpha diversity metric used to compare within sample microbiome diversity. Alpha diversity values are plotted for the following metrices: Shannon (which signifies both richness and evenness of the species in the sample). (J) Simpson. (K) Chao 1 (signify species richness in the sample). Data are expressed as mean ± SEM. Data were analyzed by unpaired Student *t* test and analyzed by one-way ANOVA. *$p \leq 0.05$, **$p \leq 0.01$, ***$p \leq 0.001$, ****$p \leq 0.0001$) compared with the indicated group.

Table 1. Demographic and clinical characteristic of human subjects.

Parameters	Healthy control (post-menopausal w/o osteoporosis)	Post-menopausal osteoporotic (PMO)	*p*-value
Age (years)	58 ± 9.78	57 ± 7.37	0.6713
BMI	26.28 ± 4.9	25.41665 ± 4.37	0.4941
T-scores spine	−0.84706 ± 0.47	−3.14615 ± 0.667	<0.0001
T-scores femur	−0.77222 ± 0.56	−2.52 ± 0.7	<0.0001
BMD at Spine (gm/cm^2)	0.953957 ± 0.16	0.70019 ± 0.09	<0.0001
BMD at femur (gm/cm^2)	0.906955 ± 0.2	0.635333 ± 0.1	<0.0001
Biochemical and Hormonal Estimations			
Vitamin D levels (ng/mL)	28.73857 ± 21.66	40.60727 ± 27.04	0.09
PTH levels (pg/mL)	59.604 ± 23.99	53.6055 ± 29	0.45
Estradiol (pg/mL)	25.94 ± 14.29	17.73 ± 4.19	0.1844

Values are represented as Mean ± SD; *p* value < 0.05 is considered as significant.

diversity) of microbial species in Ovx group (Figure 6H-K). Taken together, our results shows that IL-9 blockade enhances gut-integrity/permeability and prevents dysbiosis, thereby further lessening the burden of gut inflammation observed under postmenopausal osteoporotic conditions.

IL-9 producing Th cells are elevated in post-menopausal osteoporotic patients

We next sought to verify our pre-clinical results in post-menopausal osteoporotic patients. The clinical characteristics of the human subjects involved in the study are mentioned in the methodology section. Based on T scores, human subjects were categorized into HC (*n* = 10) and post-menopausal osteoporotic subjects (PMO, *n* = 10) (Table 1). We observed significantly increased levels of bone turnover markers (CTX-1 and osteocalcin) in the osteoporotic group compared with HC group (Figure 7A-B). Interestingly, our embedded tSNE plot immunoprofiling identified a unique cluster of IL-9 expressing Th cells in PMO subjects in comparison to HC (Figure 7C). Flow cytometry data further revealed a significant enhancement in the percentage and MFI of IL-9$^+$Th9 cells in the PBMCs of PMO compared with HC (Figure 7C-F). Interestingly we observed that the enhanced levels of IL-9$^+$Th9 cells were further positively correlated with enhanced percentage and MFI of IL-17$^+$Th17 cells in the PBMCs of PMO compared with HC (Figure 7H-J). In addition, ELISA data further demonstrated that the level of inflammatory/osteoclastogenic cytokines viz. IL-9 and IL-17 were significantly enhanced in PMO patients in comparison to the HC (Figure 7G, K). Moreover, we observed that IL-9 in a dose-dependent manner was able to significantly enhance RANKL-mediated osteoclastogenesis in human PBMCs (Figure 7L-N), thereby further indicating toward the osteoclastogenic potential of IL-9 even under clinical settings. Conclusively, both our murine and human studies found IL-9 as a key regulator of inflammatory bone loss under PMO condition.

Discussion

In 1997, Sass et al. reported that T cells are not a crucial component of bone loss observed under estrogen deficient conditions.[6] However, recent advancements revealed the pivotal role of immune system specifically T cells in the pathogenesis of osteoporosis.[10,38] Cytokines produced by Th cells play a vital role in modulating bone health under estrogen deficient

conditions.[39] The existing proinflammatory condition in Ovx mice is marked by an increase in osteoclastogenic (IL-6 and TNF-α) and concurrent decrease in anti-osteoclastogenic cytokines (IL-4, IL-10, and IFN-γ). Moreover, the observed enhancement in IL-9 levels could further worsen the inflammatory burden. The simultaneous increase in IL-9, its receptor IL-9R, and Foxo-1 that promotes the differentiation of naïve CD4$^+$ T cells toward Th9/Th17 cells suggests the possibility of a positive feedback loop, creating an auto-reinforcement. Moreover, reduction in the frequencies and migration of Th17 to the BM along with maintenance of gut-integrity and GM, post-IL-9 blockade further testify the potential of targeting IL-9 as an immunotherapy under PMO conditions.

Elevated levels of the cytokine IL-9 in the serum of RA patients promote the growth of osteoclasts, raising the possibility of blocking IL-9 as a novel approach for preserving bone health in RA patients.[26,40,41] In agreement with this, our results demonstrated that IL-9 cytokine levels were consistently elevated in Ovx mice. Further evidence that increased IL-9 levels ~~may~~ could be a pertinent factor in inflammatory bone loss under estrogen-deficient conditions comes from the fact that elevated IL-9 levels were further observed to be inversely linked with BMD. Monocytes and macrophages, the known progenitors of osteoclasts, express the greatest levels of IL-9R.[42] We too found that IL-9R expression was elevated in the BM, which promoted osteoclastogenesis and thus could be responsible for IL-9-mediated inflammatory bone loss in Ovx mice model.

Foxo-1 is a key transcription factor linked to the production of IL-9 by T helper cells in allergic asthma.[22,23,43,44] In accordance with these results, we too observed elevated levels of *foxo-1* expression in the BM in Ovx mice. This shows that the observed increase in IL-9 levels under estrogen-deficient osteoporotic situations may have involved both Th9 and Th17 cells. A renaissance of interest in IL-9 biology has resulted from the fact that multiple immune cell subsets, including Th9, Th17, Th2, Treg, and ILC2 cells, express IL-9.[45] Notably, we found that under estrogen deficient conditions, both Th9 and Th17 cells are the major source of IL-9 cytokine. This was demonstrated by the noticeably higher frequencies of IL-9$^+$IL-17$^-$Th9 cells, IL-9$^-$IL-17$^+$Th17 cells, and IL-9$^+$IL-17$^+$Th9/Th17 cells in the BM of Ovx mice. Our in vivo temporal kinetics analysis further showed that the fraction of Th cells that produced IL-9 were significantly increased in Ovx mice during progressive estrogen deprivation from days 15 to 45. Th17 cells are an established osteoclastogenic subset
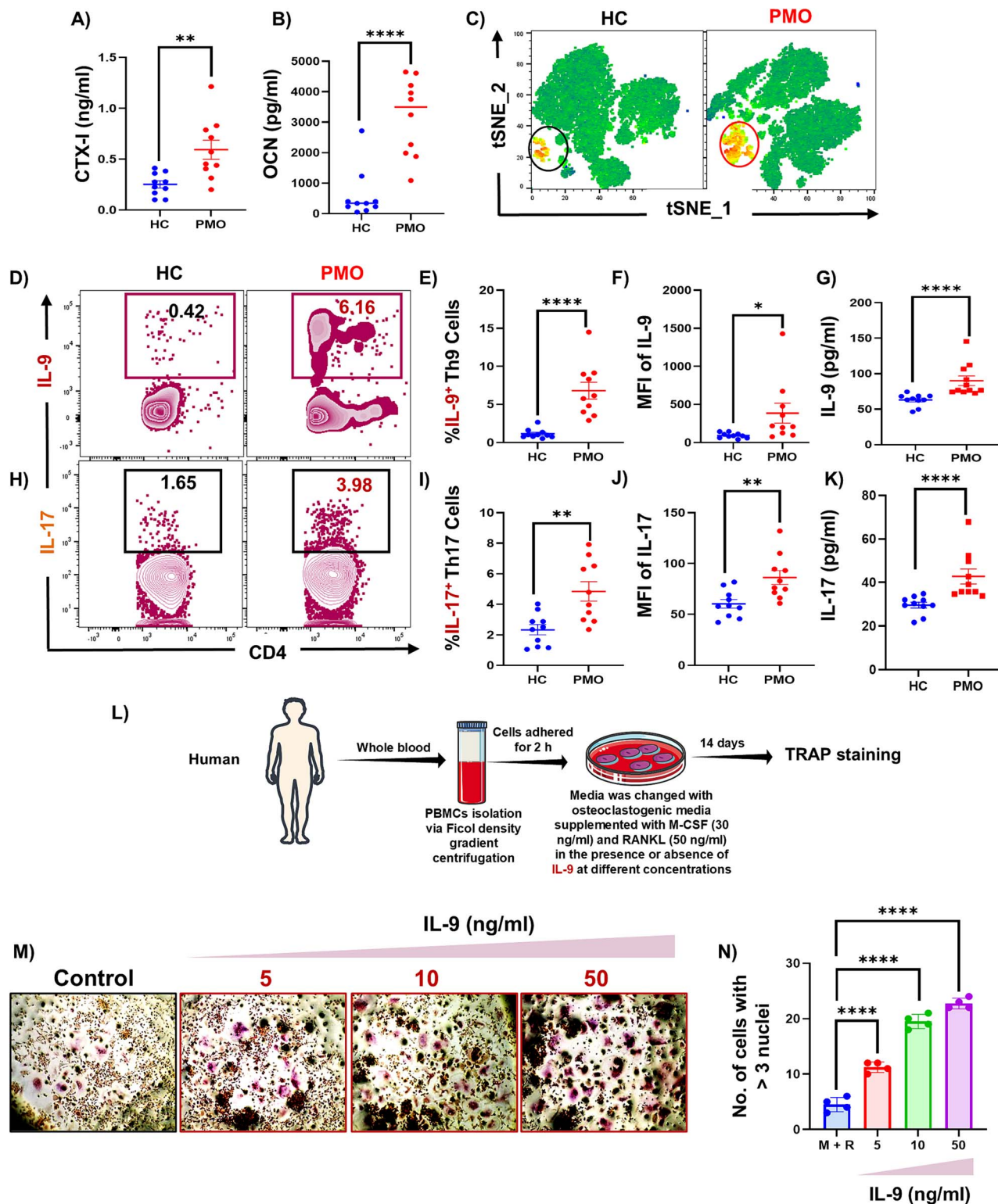
Figure 7. Th9 and Th17 cells are significantly elevated in post-menopausal osteoporotic patients: (A-B) ELISA data representing the levels of bone biochemical markers viz. CTX-1 and osteocalcin, respectively. (C) tSNE plot for the PBMCs showing expression of IL-9 cytokines gated on $CD3^+CD4^+$ Th cells. (D) Zebra plot representing the percentage of Th9 cells. (E) Plot representing the percentage of Th9 cells in control and PMO patients. (F) MFI of IL-9 in $CD4^+$ T cells in HC and PMO patients. (G) Level of IL-9 in sera of HC and PMO patients. (H) Contour plot representing the percentage of Th17 cells in control and PMO patients. (I) Plot represents the percentage of Th17 cells. (J) MFI of IL-17 in $CD4^+$ T cells in HC and PMO patients. (K) Level of IL-17 in sera of HC and PMO patients. (L) Osteoclast differentiation was induced in human PBMCs with M-CSF (25 ng/mL) and RANKL (100 ng/mL) with or without IL-9 cytokine at various concentrations for 14 d. Giant multinucleated cells were stained with TRAP and cells with ≥ 3 nuclei were considered mature osteoclasts. (M) Photomicrographs at 20× magnifications were taken. (N) Number of TRAP positive cells with more than 3 nuclei. Data are expressed as mean ± SEM. Data were analyzed by unpaired Student t test and analyzed by one-way ANOVA. $*p \leq 0.05$, $**p \leq 0.01$, $***p \leq 0.001$, $****p \leq 0.0001$ compared with the indicated group.

of Th cells but the role of Th9 cells on osteoclastogenesis is still warranted.[46] Our data demonstrated that Th9 cells significantly boost osteoclast development ex vivo in an IL-9-dependent manner, thereby showcasing themselves as the newest member to the growing family of osteoclastogenic Th cells. Notably, we further report that estrogen dampens Th9 cell's ability to induce osteoclastogenesis ex vivo.

Our findings indispensably imply that IL-9-producing Th cells contribute to inflammatory bone loss and functionally blocking IL-9 may be a novel immunotherapeutic approach to enhance bone health under estrogen-deficient environments. Anti-IL-9 therapy improved bone health by maintaining bone microarchitecture, regulating osteoclast development, and controlling the levels of bone biochemical markers, such as TRAP, RANKL, OPG, and cathepsin-K, which are linked to the process of bone remodeling.[38,46-49] Interestingly, we observed that blockade of IL-9 significantly abrogates the static histomorphometric parameters, indicating toward improved bone formation. Serum levels of PINP and CTX-1, the designated reference markers of bone formation and resorption, respectively.[50,51] Interestingly, our data indicated that blockade of IL-9 significantly enhanced the level of PINP along with concomitantly significantly reducing the levels of CTX-1 in sera of Ovx mice, indicating that IL-9 negatively impacts bone health via dysregulating the bone remodeling process. In addition, we further observed a significant reduction in osteoblastogenesis under ex vivo conditions.

Literature suggest that IL-9 plays a vital role in the development of Th17 cells.[52] Estrogen deprivation causes Th17 cells to migrate to the BM in a CCR6-CCL20 (expressed by BM stromal cells and hemopoietic cells) dependent manner.[53] IL-9 plays important role in the homing of Th17 cells to the central nervous system in experimental autoimmune encephalomyelitis (EAE),[54] thereby fueling the notion that increased IL-9 levels may be one of the major drivers of osteoclastogenic Th17 cell homing to the BM. Interestingly, we observed that in Ovx mice, IL-9 inhibition greatly decreased Th17 cell frequencies and their migration toward BM (lower expression of CCL20), which would further dampen the observed inflammatory bone loss under osteoporotic settings.

Curiously, post-IL-9 blockade, we further noticed a considerable decrease in the quantity of IL-9+Th9 cells in Ovx mice, along with a notable downregulation of IRF4 and Foxo-1 expression, which attenuated the growth of Th cells that secrete IL-9 (Th9/Th17). Our findings in the preclinical mice-model were further supported under clinical settings in PMO subjects. Both IL-9+Th9 cells and IL-17+Th17 cells in the PBMCs of PMO were significantly higher in comparison with control subjects. At the functional level, IL-9 exacerbated RANKL-induced osteoclastogenesis in both mice-BM and human-PBMCs. IL-9 blockade attenuates bone loss in Ovx mice with attendant decrease in IL-9, IL-17, and CCL-20. These cytokines may further induce osteoblasts to produce RANKL, a key cytokine that promotes osteoclast differentiation and IL-9 blockade downregulates this Ovx-induced rise in RANKL:OPG ratio. Targeting IL-9, given its position upstream in the inflammatory cascade including IL-17, CCL-20, and RANKL that leads to bone loss, represents an appealing and potentially superior strategy to existing anti-resorptive therapies, particularly denosumab (the neutralizing antibody against RANKL) that turns off the bone remodeling cycle. As a result, denosumab suffers from rapid bone turnover rebound after discontinuation leading to increased risk of multiple vertebral fractures, especially in patients who have other risk factors for fracture. Thus, neutralizing IL-9 would provide flexibility in specifically modulating the intensity and duration of inflammation without inducing toxicity in various vital organs (Figure S9A).

Claudins, Occludin, and ZO-1 are the tight junctional proteins that are expressed in the intestinal epithelial cells to form the paracellular barriers that determine the gut permeability.[55] Studies reported that leakiness in the intestinal barrier permits the translocation of microbial commensals and their associated components into the lamina propria where the activation of immune cells results in localized and systemic inflammation which is further linked with the inflammatory bone loss.[56] Adherens junctional proteins (E-cadherin and β-catenin) mediate cell–cell adhesions. Studies reported that inflammatory cytokines such as IL-6 destabilize cellular contacts and facilitate the passage of pathogens that further triggers inflammation. Unfortunately, if this destabilization is uncontrolled it may lead to the development of inflammatory conditions such as inflammatory bowel disease (IBD), inflammatory bone loss etc. Our immunofluorescence data revealed that IL-9 via reducing the expression of these tight and adherens junctional proteins induce the destabilization of epithelial monolayer in a dose dependent manner. Reduction in the gut-integrity/permeability is further attested by the decreased translation of FITC labeled inulin from apical side toward the basal side of the epithelial Caco2 cell monolayer. Altogether, these data suggest toward the potent role of IL-9 in inducing the disruption of gut-intestinal barrier.

Estrogen deficiency compromises gut-integrity.[57] Fascinatingly, our data reported that under estrogen deficient conditions enhanced levels of IL-9 were further correlated with the compromised gut-integrity (significant reduction in the expression of claudin and occludin), which was significantly restored with IL-9 blockade. GM influences bone metabolism via its effect on the host immune, endocrine, and gut systems. The GM is altered at multiple taxonomic levels in patients with IBD[58] and osteoporosis. Thus, targeting GM with novel therapeutic approaches can help in preventing bone loss in osteoporosis. Interestingly, we observed that alterations in the alpha (richness and evenness) diversity in Ovx mice were significantly reversed with IL-9 blockade. Altogether, our findings demonstrate the multidimensional role of IL-9 in the pathophysiology of osteoporosis.

In the current study, we identified the mechanisms by which IL-9 could influence bone health under estrogen-deficient condition. It is still unclear if Th9, in the absence of Th17, can cause bone loss. While our current findings demonstrate the presence of IL-9+IL-17+ Th cells in the BM of Ovx mice, future studies are required to delineate the precise regulatory influence of these immune cell populations in PMO. Additionally, we demonstrated that IL-9 modulates osteoclastogenesis in an RANKL-dependent manner. As various osteoclastogenic/anti-osteoclastogenic cytokines act via the JAK/STAT signaling pathway,[59] it would be important to study whether IL-9 mediates its anti-osteoclastogenic action by this pathway. In addition, validating the skeletal effects of IL-9 in appropriate transgenic mice models is required.

In summary, our study offers the first clinically relevant evidence of the osteoclastogenic properties of Th9 cells, which are mediated by IL-9 (Graphical Abstract). Both our preclinical and clinical data substantiate Th9 cell's osteoclastogenic and osteoporotic functions under estrogen-deficient

conditions, thereby proposing Th9 as the newest member to the expanding list of osteoclastogenic T helper subsets. These results thereby highlight the revolutionary relevance of "Th9/IL-9" axis as a promising immunotherapeutic target for the management and treatment of inflammatory bone loss observed in PMO via modulating the "Gut-Immune-Bone" axis.

Author contributions

R.K.S.: conceptualization, methodology, validation, formal analysis, resources, writing original draft, visualization, supervision, project administration and funding acquisition. L.S.: Data curation, writing original draft, investigation, and formal analysis. C.S.: Data curation and formal analysis. A.S.M., S.S., D.N. and P.K.M.: methodology and formal analysis. N.C.: methodology, writing-review and editing and formal analysis. B.G., V.M., S.G. and A.N.: methodology. Leena Sapra (Data curation, Formal analysis, Investigation, Writing—original draft), Chaman Saini (Data curation, Formal analysis), Shivani Sharma (Methodology), Dibyani Nanda (Methodology), Aishwarya Nilakhe (Methodology), Naibedya Chattopadhyay (Formal analysis, Methodology, Writing—review & editing), Avtar Singh Meena (Formal analysis, Methodology), Pradyumna K. Mishra (Formal analysis, Methodology), Sarika Gupta (Formal analysis, Methodology), Bhavuk Garg (Resources), Vikrant Manhas (Resources), and Rupesh K. Srivastava (Conceptualization, Formal analysis, Funding acquisition, Investigation, Methodology, Project administration, Resources, Supervision, Validation, Visualization, Writing—original draft, Writing—review & editing).

Supplementary material

Supplementary material is available at *JBMR Plus* online.

Conflicts of interest

None declared.

Data availability

The data that support the findings of this study are available on request from the corresponding author.

References

1. Warriner AH, Patkar NM, Curtis JR, et al. Which fractures are most attributable to osteoporosis? *J Clin Epidemiol [Internet]*. 2011;64(1):46-53. Available from:. https://linkinghub.elsevier.com/retrieve/pii/S0895435610002635
2. Khosla S. Pathogenesis of age-related bone loss in humans. *J Gerontol A Biol Sci Med Sci*. 2013;68(10):1226-1235. https://doi.org/10.1093/gerona/gls163
3. Shen Y, Huang X, Wu J, et al. The global burden of osteoporosis, low bone mass, and its related fracture in 204 countries and territories, 1990-2019. *Front Endocrinol (Lausanne) [Internet]*. 2022;13:117253. Available from: https://doi.org/https://www.frontiersin.org/articles/10.3389/fendo.2022.882241/full
4. Pfeilschifter J, Köditz R, Pfohl M, Schatz H. Changes in proinflammatory cytokine activity after menopause. *Endocr Rev*. 2002;23(1):90-119. Available from: https://doi.org/10.1210/edrv.23.1.0456. https://academic.oup.com/edrv/article/23/1/90/2424228
5. Straub RH. The complex role of estrogens in inflammation. *Endocr Rev*. 2007;28(5):521-574. Available from: https://doi.org/10.1210/er.2007-0001. https://academic.oup.com/edrv/article/28/5/521/2355015
6. Sass DA, Liss T, Bowman AR, et al. The role of the T-lymphocyte in estrogen deficiency osteopenia. *JBMR Plus*. 1997;12(3):479-486. Available from: https://doi.org/10.1359/jbmr.1997.12.3.479. https://academic.oup.com/jbmr/article/12/3/479-486/7514297
7. Lee S-K, Kalinowski JF, Jacquin C, Adams DJ, Gronowicz G, Lorenzo JA. Interleukin-7 influences osteoclast function in vivo but is not a critical factor in ovariectomy-induced bone loss. *J Bone Miner Res [Internet]*. 2006;21(5):695-702. Available from: https://academic.oup.com/jbmr/article/21/5/695-702/7593347
8. Anginot A, Dacquin R, Mazzorana M, Jurdic P. Lymphocytes and the Dap12 adaptor are key regulators of osteoclast activation associated with gonadal failure. Nixon D, editor. *PLoS One [Internet]*. 2007;2(7):e585. Available from: https://dx.plos.org/10.1371/journal.pone.0000585
9. Srivastava RK, Dar HY, Mishra PK. Immunoporosis: immunology of osteoporosis—role of T cells. *Front Immunol [Internet]*. 2018;9:657. Available from: http://journal.frontiersin.org/article/10.3389/fimmu.2018.00657/full
10. Srivastava RK, Sapra L. The rising era of "Immunoporosis": role of immune system in the pathophysiology of osteoporosis. *J Inflamm Res [Internet]*. 2022;15:1667-1698. Available from: 10.2147/JIR.S351918. https://www.dovepress.com/the-rising-era-of-immunoporosis-role-of-immune-system-in-the-pathophys-peer-reviewed-fulltext-article-JIR
11. Sapra L, Azam Z, Rani L, et al. "Immunoporosis": immunology of osteoporosis. *Proc Natl Acad Sci India Sect B Biol Sci [Internet]*. 2021;91(3):511-519. Available from: https://link.springer.com/10.1007/s40011-021-01238-x
12. Cenci S, Weitzmann MN, Roggia C, et al. Estrogen deficiency induces bone loss by enhancing T-cell production of TNF-α. *J Clin Invest [Internet]*. 2000;106(10):1229-1237. Available from: http://www.jci.org/articles/view/11066
13. Cenci S, Toraldo G, Weitzmann MN, et al. Estrogen deficiency induces bone loss by increasing T cell proliferation and lifespan through IFN-γ-induced class II transactivator. *Proc Natl Acad Sci [Internet]*. 2003;100(18):10405-10410. Available from: https://pnas.org/doi/full/10.1073/pnas.1533207100
14. Zhang W, Dang K, Huai Y, Qian A. Osteoimmunology: the regulatory roles of T lymphocytes in osteoporosis. *Front Endocrinol (Lausanne). [Internet]*. 2020;11:465. Available from: https://www.frontiersin.org/article/10.3389/fendo.2020.00465/full
15. Pacifici R. Role of T cells in ovariectomy induced bone loss—revisited. *J Bone Miner Res*. 2012;27(2):231-239. https://doi.org/10.1002/jbmr.1500
16. Roggia C, Gao Y, Cenci S, et al. Up-regulation of TNF-producing T cells in the bone marrow: a key mechanism by which estrogen deficiency induces bone loss in vivo. *Proc Natl Acad Sci [Internet]*. 2001;98(24):13960-13965. Available from: https://pnas.org/doi/full/10.1073/pnas.251534698
17. Lehmann J, Thiele S, Baschant U, et al. Mice lacking DKK1 in T cells exhibit high bone mass and are protected from estrogen-deficiency-induced bone loss. *iScience [Internet]*. 2021;24(3):102224. Available from: https://doi.org/10.1016/j.isci.2021.102224. https://linkinghub.elsevier.com/retrieve/pii/S2589004221001929
18. Pacifici R. T cells and post menopausal osteoporosis in murine models. *Arthritis Res Ther [Internet]* 2007;9(2):102. Available from: https://doi.org/https://doi.org/10.1186/ar2126

19. Yu M, Malik Tyagi A, Li J-Y, et al. PTH induces bone loss via microbial-dependent expansion of intestinal TNF+ T cells and Th17 cells. *Nat Commun [Internet]*. 2020;11(1):468. Available from: http://www.nature.com/articles/s41467-019-14148-4

20. Veldhoen M, Uyttenhove C, van Snick J, et al. Transforming growth factor-*β* "reprograms" the differentiation of T helper 2 cells and promotes an interleukin 9–producing subset. *Nat Immunol [Internet]*. 2008;9(12):1341-1346. Available from: https://www.nature.com/articles/ni.1659

21. Staudt V, Bothur E, Klein M, et al. Interferon-regulatory factor 4 is essential for the developmental program of T helper 9 cells. *Immunity* 2010. 33(2):192–202. Available from: https://linkinghub.elsevier.com/retrieve/pii/S1074761310002797 https://doi.org/10.1016/j.immuni.2010.07.014

22. Malik S, Sadhu S, Elesela S, et al. Transcription factor Foxo1 is essential for IL-9 induction in T helper cells. *Nat Commun [Internet]*. 2017;8(1):815. Available from: https://doi.org/10.1038/s41467-017-00674-6. https://www.nature.com/articles/s41467-017-00674-6

23. Malik S, Awasthi A. Transcriptional control of Th9 cells: role of Foxo1 in interleukin-9 induction. *Front Immunol [Internet]*. 2018;9:995. Available from: https://doi.org/10.3389/fimmu.2018.00995

24. Licona-Limón P, Henao-Mejia J, Temann AU, et al. Th9 cells drive host immunity against gastrointestinal worm infection. *Immunity [Internet]*. 2013;39(4):744-757 Available from: https://linkinghub.elsevier.com/retrieve/pii/S1074761313004342

25. Li J, Chen S, Xiao X, Zhao Y, Ding W, Li XC. IL-9 and Th9 cells in health and diseases—from tolerance to immunopathology. *Cytokine Growth Factor Rev [Internet]*. 2017;37:47-55. Available from: https://linkinghub.elsevier.com/retrieve/pii/S1359610117301090

26. Ciccia F, Guggino G, Rizzo A, et al. Potential involvement of IL-9 and Th9 cells in the pathogenesis of rheumatoid arthritis. *Rheumatology [Internet]* 2015; 54(12):2264–2272. Available from: https://academic.oup.com/rheumatology/article-lookup/doi/10.1093/rheumatology/kev252

27. Lyu Z, Hu Y, Guo Y, Liu D. Modulation of bone remodeling by the gut microbiota: a new therapy for osteoporosis. *Bone Res [Internet]*. 2023;11(1):31. Available from: https://www.nature.com/articles/s41413-023-00264-x

28. Bhardwaj A, Sapra L, Tiwari A, Mishra PK, Sharma S, Srivastava RK. "Osteomicrobiology": the nexus between bone and bugs. *Front Microbiol [Internet]*. 2022;12:812466. Available from: https://www.frontiersin.org/articles/10.3389/fmicb.2021.812466/full

29. Sapra L, Dar HY, Bhardwaj A, et al. Lactobacillus rhamnosus attenuates bone loss and maintains bone health by skewing Treg-Th17 cell balance in Ovx mice. *Sci Rep [Internet]*. 2021;11(1):1807. Available from: http://www.nature.com/articles/s41598-020-80536-2

30. Tian L, Li Y, Zhang J, Chang R, Li J, Huo L. IL-9 promotes the pathogenesis of ulcerative colitis through STAT3/SOCS3 signaling. *Biosci Rep [Internet]* 2018; 38(6):BSR20181521. Available from: https://portlandpress.com/bioscirep/article/38/6/BSR20181521/98273/IL-9-promotes-the-pathogenesis-of-ulcerative, 10.1042/BSR20181521

31. Sun J-K, Zhou J, Sun X-P, et al. Interleukin-9 promotes intestinal barrier injury of sepsis: a translational research. *J Intensive Care [Internet]*. 2021;9(1):37. Available from: https://jintensivecare.biomedcentral.com/articles/10.1186/s40560-021-00550-y

32. Vyas SP, Goswami R. A decade of Th9 cells: role of Th9 cells in inflammatory bowel disease. *Front Immunol [Internet]*. 2018;9:1139. Available from: https://www.frontiersin.org/article/10.3389/fimmu.2018.01139/full

33. Sapra L, Shokeen N, Porwal K, et al. Bifidobacterium longum ameliorates ovariectomy-induced bone loss via enhancing anti-osteoclastogenic and immunomodulatory potential of regulatory B cells (Bregs). *Front Immunol [Internet]*. 2022;13:875788.

Available from: https://www.frontiersin.org/articles/10.3389/fimmu.2022.875788/full

34. Sapra L, Dar HY, Bhardwaj A, et al. Lactobacillus rhamnosus attenuates bone loss and maintains bone health by skewing Treg-Th17 cell balance in Ovx mice. *Sci Rep [Internet]*. 2021;11(1):1807. Available from: https://www.nature.com/articles/s41598-020-80536-2

35. Sapra L, Shokeen N, Porwal K, et al. Bifidobacterium longum ameliorates ovariectomy-induced bone loss via enhancing anti-osteoclastogenic and immunomodulatory potential of regulatory B cells (Bregs). *Front Immunol*. 2022;13:1-19.

36. Chen R-Y, Fan Y-M, Zhang Q, et al. Estradiol inhibits Th17 cell differentiation through inhibition of ROR*γ*T transcription by recruiting the ER*α*/REA complex to estrogen response elements of the ROR*γ*T promoter. *J Immunol [Internet]*. 2015;194(8):4019-4028. Available from: https://journals.aai.org/jimmunol/article/194/8/4019/104564/Estradiol-Inhibits-Th17-Cell-Differentiation

37. Ohlsson C, Sjögren K. Osteomicrobiology: a new cross-disciplinary research field. *Calcif Tissue Int*. 2018;102(4):426-432.

38. Srivastava RK, Dar HY, Mishra PK. Immunoporosis: immunology of osteoporosis—role of T cells. *Front Immunol [Internet]*. 2018;9:657. Available from: http://journal.frontiersin.org/article/10.3389/fimmu.2018.00657/full

39. Amarasekara DS, Yu J, Rho J. Bone loss triggered by the cytokine network in inflammatory autoimmune diseases. *J Immunol Res [Internet]*. 2015;116:1-12, 154875. Available from: http://www.hindawi.com/journals/jir/2015/832127/

40. Kar S, Gupta R, Malhotra R, et al. Interleukin-9 facilitates osteoclastogenesis in rheumatoid arthritis. *Int J Mol Sci [Internet]*. 2021;22(19):10397. Available from: https://www.mdpi.com/1422-0067/22/19/10397

41. Chakraborty S, Schneider J, Mitra DK, Kubatzky KF. Mechanistic insight of interleukin-9 induced osteoclastogenesis. *Immunology [Internet]*. 2023;169(3):309-322 Available from: https://onlinelibrary.wiley.com/doi/10.1111/imm.13630

42. Donninelli G, Saraf-Sinik I, Mazziotti V, et al. Interleukin-9 regulates macrophage activation in the progressive multiple sclerosis brain. *J Neuroinflammation [Internet]*. 2020;17(1):149. Available from: https://jneuroinflammation.biomedcentral.com/articles/10.1186/s12974-020-01770-z

43. Buttrick TS, Wang W, Yung C, et al. Foxo1 promotes Th9 cell differentiation and airway allergy. *Sci Rep [Internet]*. 2018;8(1):818. Available from: https://www.nature.com/articles/s41598-018-19315-z

44. Bi E, Ma X, Lu Y, et al. Foxo1 and Foxp1 play opposing roles in regulating the differentiation and antitumor activity of T H 9 cells programmed by IL-7. *Sci Signal [Internet]*. 2017;10(500) Available from: https://www.science.org/doi/10.1126/scisignal.aak9741

45. Nowak EC, Noelle RJ. Interleukin-9 as a T helper type 17 cytokine. *Immunology [Internet]*. 2010;131(2):169-173 Available from: https://onlinelibrary.wiley.com/doi/10.1111/j.1365-2567.2010.03332.x

46. Tyagi AM, Srivastava K, Mansoori MN, Trivedi R, Chattopadhyay N, Singh D. Estrogen deficiency induces the differentiation of IL-17 secreting Th17 cells: a new candidate in the pathogenesis of osteoporosis. Frey O, editor. *PLoS One [Internet]*. 2012;7(9):e44552. Available from: https://dx.plos.org/10.1371/journal.pone.0044552

47. Sato K, Suematsu A, Okamoto K, et al. Th17 functions as an osteoclastogenic helper T cell subset that links T cell activation and bone destruction. *J Exp Med [Internet]*. 2006;203(12):2673-2682. Available from: https://rupress.org/jem/article/203/12/2673/46311/Th17-functions-as-an-osteoclastogenic-helper-T

48. Tsukasaki M, Takayanagi H. Osteoimmunology: evolving concepts in bone–immune interactions in health and disease. *Nat Rev Immunol [Internet]*. 2019;19(10):626-642. Available from: http://www.nature.com/articles/s41577-019-0178-8

49. Dar HY, Azam Z, Anupam R, Mondal RK, Srivastava RK. Osteoimmunology: the nexus between bone and immune system. *Front Biosci (Landmark Ed)*. 2018;23(3):464-492. Available from: http://www.ncbi.nlm.nih.gov/pubmed/28930556

50. Gillet M, Vasikaran S, Inderjeeth C. The role of PINP in diagnosis and management of metabolic bone disease. *Clin Biochem Rev [Internet]*. 2021;42(1):3-10. Available from: https://www.aacb.asn.au/clinical-biochemist-reviews/area?command=record&id=326&cid=36

51. Anwar A, Sapra L, Gupta N, Ojha RP, Verma B, Srivastava RK. Fine-tuning osteoclastogenesis: an insight into the cellular and molecular regulation of osteoclastogenesis. *J Cell Physiol*. 2023;238(7):1431-1464.

52. Elyaman W, Bradshaw EM, Uyttenhove C, et al. IL-9 induces differentiation of T H 17 cells and enhances function of FoxP3 + natural regulatory T cells. *Proc Natl Acad Sci [Internet]*. 2009;106(31):12885-12890. Available from: https://pnas.org/doi/full/10.1073/pnas.0812530106

53. Yu M, Pal S, Paterson CW, et al. Ovariectomy induces bone loss via microbial-dependent trafficking of intestinal TNF+ T cells and Th17 cells. *J Clin Invest [Internet]* 2021; 131(4). Available from: https://www.jci.org/articles/view/143137, 10.1172/JCI143137

54. Zhou Y, Sonobe Y, Akahori T, et al. IL-9 promotes Th17 cell migration into the central nervous system via CC chemokine ligand-20 produced by astrocytes. *J Immunol [Internet]*. 2011;186(7):4415-4421. Available from: https://journals.aai.org/jimmunol/article/186/7/4415/85298/IL-9-Promotes-Th17-Cell-Migration-into-the-Central

55. Günzel D, Yu ASL. Claudins and the modulation of tight junction permeability. *Physiol Rev [Internet]*. 2013;93(2):525-569. Available from: https://www.physiology.org/doi/10.1152/physrev.00019.2012

56. Schepper JD, Collins F, Rios-Arce ND, et al. Involvement of the gut microbiota and barrier function in glucocorticoid-induced osteoporosis. *J Bone Miner Res [Internet]*. 2020;35(4):801-820. Available from: https://academic.oup.com/jbmr/article/35/4/801/7516507

57. Baker JM, Al-Nakkash L, Herbst-Kralovetz MM. Estrogen–gut microbiome axis: physiological and clinical implications. *Maturitas [Internet]*. 2017;103:45-53 Available from: https://linkinghub.elsevier.com/retrieve/pii/S0378512217306503

58. Hufford MM, Kaplan MH. A gut reaction to IL-9. *Nat Immunol [Internet]*. 2014;15(7):599-600. Available from: https://www.nature.com/articles/ni.2916

59. Xu J, Yu L, Liu F, Wan L, Deng Z. The effect of cytokines on osteoblasts and osteoclasts in bone remodeling in osteoporosis: a review. *Front Immunol [Internet]*. 2023;14. Available from: https://www.frontiersin.org/articles/10.3389/fimmu.2023.1222129/full